An Improved *LCLC* Current-Source-Output Multistring LED Driver With Capacitive Current Balancing

Xiaohui Qu, *Member, IEEE*, Siu-Chung Wong, *Senior Member, IEEE*, and Chi K. Tse, *Fellow, IEEE*

***Abstract*—Passive or active current balancing circuits are usually used to mitigate current imbalance in driving multiple light-emitting-diode (LED) strings. Passive current balancing schemes adopting capacitors with high reliability, small size and low cost are very popular in many applications. However, the high reactive power of the capacitive balancing scheme with variable frequency control will bring high power stress on the VA rating of the main switches which drive this passive current balancing circuit and decrease the overall efficiency. Fixed frequency control does not permit zero-voltage switching (ZVS) under load variations. Hence, this paper proposes a current-source-output LED driver based on *LCLC* resonant circuit to provide a constant output current regardless of variations in LED parameters. In the *LCLC* circuit, the number of additional capacitors is scalable with the number of LED strings for current balancing. Moreover, the input impedance of the improved *LCLC* circuit is designed to be resistive at the operating frequency to minimize reactive power. The conventional duty cycle control can easily incorporate ZVS. The analysis, implementation and verification are detailed in this paper.**

***Index Terms*—Constant current source, current balancing, light-emitting-diode (LED) driver, passive circuit.**

I. Introduction

With the development of light-emitting-diode (LED) devices for general lighting applications, LED manufacturers have focused on high-brightness high-power LED products to cope with the market trend [1]. For a better thermal design, an LED package usually has a power of less than 5 W per chip. Thus, a single LED package cannot emit enough luminance for general lighting applications. Therefore, several LEDs are usually connected together for various LED applications such as LCD back lighting, streetlight, general lighting, etc., [2], [3].

A single *LED load* can be economically driven by a single driver. Thus, LEDs are mostly connected in parallel with several LED strings. Each LED string is formed by connecting several LEDs in series for a safe accumulative forward voltage. However, LED *V–I* characteristic inherently follows a statistical manufacturing spread and varies with temperature. Unequal current in each LED string is expected when a number of paralleled LED strings are connected to a common voltage terminal as a single load. Without current balancing mechanism, high current can be developed in some LED strings which will be rapidly degraded or will even fail. Therefore, many techniques have been developed to mitigate the current imbalance.

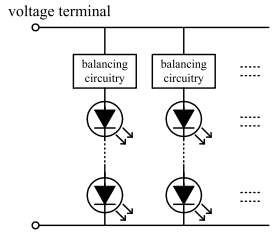

Fig. 1. LED load with balancing circuitry for each LED string.

The current imbalance of LED strings within an LED load is caused by unequal *V–I* curves of LED strings. To balance currents in multiple LED strings simultaneously, additional balancing circuitry must be inserted within the LED load to regulate the current and absorb the voltage difference in each LED string, as shown in Fig. 1. The balancing circuitry can be passive or active. Active balancing circuitry includes switched current regulator [4]–[7], linear regulator, current mirror [8] and so on. Obviously, linear regulators and current mirrors are simple and economical to implement, but the losses on the linear transistors are relatively high. The switched current regulator uses high-frequency on-off switches to control current of each LED string with high efficiency. However, the switched-mode circuit and control logic are complex and less reliable. Recently, some attempts have been made to improve the efficiency of linear schemes with the penalty of complex control [9]–[11]. In the passive balancing circuit, lossy resistors are not considered in high-power LED applications. The inductor and capacitor without real power dissipation are good candidates. The ac currents from a pair of coupled inductors with 1:1 turns ratio [12] or from two complementary rectified current paths of an ac capacitor [13]–[16] can automatically balance the currents of two LED strings according to the principles of electromagnetic induction and capacitive charge balance, as shown in Fig. 2. It should be noted that each LED string in capacitive charge balance shares the ac current alternatively for half a period by using two additional semicontrolled diodes. The coupled inductors

Manuscript received August 18, 2014; revised October 31, 2014; accepted November 24, 2014. Date of publication December 4, 2014; date of current version May 22, 2015. This work was supported by the National Natural Science Foundation of China under Grant 51107009, the Natural Science Foundation of Jiangsu Province under Grant BK20141339, and Hong Kong RGC under theme-based Research Project T22-715/12-N. Recommended for publication by Associate Editor J. M. Alonso.

X. Qu is with the School of Electrical Engineering, Southeast University, Nanjing 210096, China (e-mail: xhqu@seu.edu.cn).

S.-C. Wong and C. K. Tse are with the Department of Electronic and Information Engineering, Hong Kong Polytechnic University, Hong Kong (e-mail: enscwong@polyu.edu.hk; encktse@polyu.edu.hk).

Color versions of one or more of the figures in this paper are available online at http://ieeexplore.ieee.org.

Digital Object Identifier 10.1109/TPEL.2014.2377244

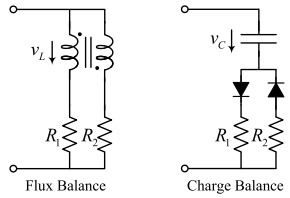

Fig. 2. Inductive flux balance and capacitive charge balance with two LED strings.

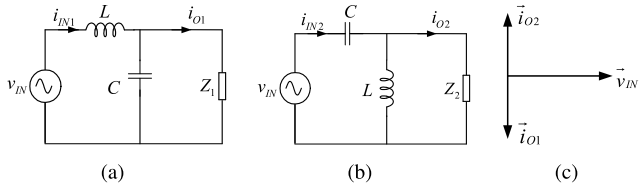

Fig. 3. Two parallel resonant circuits of (a) and (b) with the corresponding vectors of input voltage $\vec{v}_{\rm IN}$ and output currents $\vec{i}_{O1}$ and $\vec{i}_{O2}$ in (c).

and the capacitor within the charge balancing circuitry also act as voltage snubbers to absorb the voltage difference between two LED strings. To balance currents for more LED strings, the number of coupled inductor will increase exponentially and the number of LED strings having balanced current must be an even number [17]–[19]. It has been previously proposed to reduce the number of coupled inductors with diploid relation to the number of LED strings and hence eliminate the strict requirement of an even number of balancing strings [20]. Capacitive charge balance also has similar limitation of only balancing an even number of LED strings. However, implementation of capacitive charge balance is complicated if the number of LED strings is more than two because every two LED strings need a capacitor and some fully controlled switches to facilitate the complementary conduction paths [21]. Generally, the inductive flux balance scheme suffers from low power density and high production cost compared to the capacitive scheme. The capacitive charge balance scheme is hard to implement for multiple LED strings. As a tradeoff, a hybrid structure with coupled inductor and blocking capacitor has been used [21], [22].

Unlike the balancing circuitries in Fig. 2, near identical current can be achieved by using a reactance in series with the resistive LED string[23], [24], provided that the reactance is sufficiently larger than the equivalent resistance of each LED string. The differences among the LED equivalent resistances can be neglected and a small current variation among LED strings can be guaranteed. However, direct driving this large reactance brings large reactive power, which will increase the VA rating and decrease the overall efficiency of the LED driver. Alternatively, the reactive loads can be driven indirectly with an opposite reactance to form a resonant tank. At the operating frequency, the impedance of the LED load can be compensated to be resistive for direct driving with minimal power stress. To supply the required current for the LED load, frequency control and/or pulse-width-modulation (PWM) control can be used. It is well known that LED has nonlinear characteristics and the equivalent resistance varies with driving current and junction temperature. Even when driven at a constant current, LED forward voltage still drifts nonlinearly with temperature. In some LED back lighting panels, the number of LEDs in one string is not fixed. The wide load range will widen the frequency variation and/or duty cycle variation, increase the reactive power, and make it difficult for converter optimization. A control using a hybrid of frequency and PWM has been used to prevent the wide variations of these two control variables with improved performance [25]. However, the control is complex.

Based on the aforementioned analysis, this paper proposes a current-source-output LED driver based on an *LCLC* resonant circuit which decouples the effect of load variation from the output current. The *LCLC* circuit can be improved with a capacitive balancing scheme to realize the current balancing for multiple LED strings. The *LCLC* circuit can also be designed with zero input reactive power at the operating frequency. Then, duty cycle control at the operating frequency can be adopted for the required current with zero-voltage switching (ZVS). As an output current source, the proposed LED driver is inherently LED-side short-circuit proof, and PWM dimming can be easily implemented. The proposed LED driver is simple, reliable, economical and efficient for multiple LED string applications. Section II gives the basic concept and derivation of the proposed LED driver. The detailed analysis of circuit design, control and implementation is given in Section III. The performance of the proposed LED driver is evaluated in Section IV. Section V concludes the paper.

II. Basic Concept of the Proposed LED Driver

A. Resonant Circuits With Constant Output Current and Zero Input Phase Angle

To simplify the control, the LED driver should operate as a constant current source independent of load variation. With the abundant supply of voltage source, a pure sinusoidal ac voltage driven parallel resonant tank as shown in Fig. 3 can facilitate the transformation of the ac voltage source $v_{\rm IN}$ to an ac current source i_{Oi} to drive the load Z_i, where $i = 1$ or 2.

We use a frequency-domain analysis of the circuit for simplicity. When $v_{\rm IN}$ operates at $f_r = \frac{1}{2\pi\sqrt{LC}}$, it can be readily shown that the output current is a constant given by

$$i_{O1} = -v_{\rm IN} \cdot j\omega_r C \ \text{ and } \ i_{O2} = -\frac{v_{\rm IN}}{j\omega_r L} \tag{1}$$

where $\omega_r = 2\pi f_r$. As indicated in Fig. 3(c), i_{O1} and i_{O2} have the same magnitude and are out of phase that they are load independent. The parallel resonant circuits are inherently output short-circuit proof. However, output open-circuit is prohibited and an output open-circuit protection circuit should be implemented.

In a practical implementation, $v_{\rm IN}$ is generated from a full-bridge or half-bridge switching circuit. The reactive power and circuit VA rating of the switching circuit should be minimized. Effectively, the input impedance of the reactive elements should be resistive. Now, the input impedances of these two circuits are

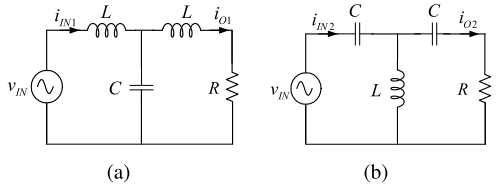

Fig. 4. Circuits with constant output current and input ZPA: (a) LCL-T type and (b) CLC-T type.

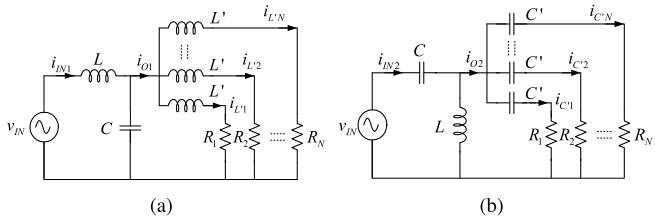

Fig. 5. Improved circuits with constant output current, input ZPA and reactive current balancing scheme: (a) LCL-T type and (b) CLC-T type.

investigated as

$$Z_{\mathrm{IN}1} = \frac{v_{\mathrm{IN}}}{i_{\mathrm{IN}1}} = j\omega_r L + \frac{1}{j\omega_r C} \parallel Z_1 = \frac{\frac{L}{C}}{\frac{1}{j\omega_r C} + Z_1} \text{ and} \quad (2)$$

$$Z_{\mathrm{IN}2} = \frac{v_{\mathrm{IN}}}{i_{\mathrm{IN}2}} = \frac{1}{j\omega_r C} + j\omega_r L \parallel Z_2 = \frac{\frac{L}{C}}{j\omega_r L + Z_2}. \quad (3)$$

Impedances $Z_{\mathrm{IN}1}$ and $Z_{\mathrm{IN}2}$ are resistive if $Z_1 = j\omega_r L$ in (2), and $Z_2 = \frac{1}{j\omega_r C}$ in (3). So, additional inductive or capacitive component is added in these two parallel resonant circuits to realize the input zero-phase-angle (ZPA), as shown in Fig. 4. As a result, the input impedances in (2) and (3) become

$$Z_{\mathrm{IN}} = \frac{v_{\mathrm{IN}}}{i_{\mathrm{IN}1}} = \frac{v_{\mathrm{IN}}}{i_{\mathrm{IN}2}} = \frac{L}{\mathrm{RC}}. \quad (4)$$

B. Integration With Current Balancing Schemes

In Section II-A, we have shown that the LCL-T and CLC-T circuits operating at f_r can output a constant ac current and can be driven with zero reactive power. Each LED string driven by one of these two circuits with the same parameters can have near identical current. In [26], multiple LCL-T circuits are used and connected to a common ac line to realize the current balancing for multiple LED strings. One LED string requires an LCL-T circuit, which is easy for a modular design. However, the component tolerances of the LCL-T circuit affect the accuracy of the output current for each LED string and the power density with each LED string having an LCL-T module is relatively low.

To improve the current balancing performance and power density, the existing large reactance balancing schemes can be integrated within the LCL-T and CLC-T circuits for current balancing. The basic concept is to duplicate the output inductor or capacitor with LED strings in the resonant tank, but keeping the overall reactance the same, as shown in Fig. 5. With a much larger reactance of L' or C' than the equivalent LED string loading resistance $R_m, m \in 1, 2, \cdots, N$, each LED string connected with the same L' or C' can equally share the constant output current i_{O1} or i_{O2}. To ensure ZPA, the overall reactance should equal to that as in Fig. 4, i.e.

$$L' = NL \text{ and } C' = \frac{C}{N} \quad (5)$$

$$i_{L'1} = i_{L'2} = \cdots = i_{L'N} = \frac{i_{O1}}{N} \quad (6)$$

$$i_{C'1} = i_{C'2} = \cdots = i_{C'N} = \frac{i_{O2}}{N}. \quad (7)$$

Here, N can be odd or even. Compared with the current balancing scheme in [26], the improved current balancing scheme based on an LCL-T or CLC-T circuit only needs one pair of *LC* or *CL* and N balancing inductors or capacitors to realize N balanced and constant LED current, which saves $N-1$ pairs of *LC* or *CL*. The accuracy of current balance is affected only by the tolerances of N balancing inductors or capacitors.

The tolerance distribution of inductors is determined by the production process. Obviously, an LCL-T circuit with N larger inductors L' will decrease the power density and increase the production cost. The use of coupled inductors will face the original problem of inductive flux balance. Therefore, the CLC-T circuit will be adopted for the subsequent development. The tolerance of film capacitors is normally $\pm 5\%$. As the total output current i_{O2} is determined by the leading *CL* impedances, the tolerances of balancing capacitors and load resistors will not affect the accuracy of i_{O2}. Assuming the tolerance of C'_p is α_p, where the subscript $p \in \{1, 2, \cdots, N\}$ denotes the index of LED strings, we have

$$C'_p = C'(1 + \alpha_p) \quad (8)$$

$$i_{C'1} \cdot \frac{1}{j\omega C'_1} = i_{C'2} \cdot \frac{1}{j\omega C'_2} = \cdots = i_{C'N} \cdot \frac{1}{j\omega C'_N} \quad (9)$$

$$i_{O2} = i_{C'1} + i_{C'2} + \cdots + i_{C'N}. \quad (10)$$

The current deviation d_p can be calculated by

$$d_p = \frac{\left|i_{C'p} - \frac{i_{O2}}{N}\right|}{\frac{i_{O2}}{N}} = \frac{\left|N\alpha_p - \sum_{i=1}^{N} \alpha_i\right|}{N + \sum_{i=1}^{N} \alpha_i}. \quad (11)$$

Besides the integration with reactive current balancing, CLC-T circuit with N capacitors C' can be easily realized with current balancing in $2N$ LED strings by further incorporating the charge balance scheme in Fig. 6. Diodes are needed to ensure two LED strings connected with a capacitor conducting alternatively for half a period.

III. Circuit Design, Control and Implementation

From the aforementioned analysis, the improved CLC-T circuit combined with the reactive current balancing scheme in Fig. 5(b) features constant output current, zero input reactive power and output current balancing for arbitrary resistances of LED load strings. If the number of load strings is even, the

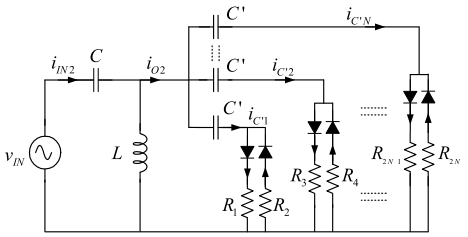

Fig. 6. Improved CLC-T circuit of Fig. 5(b) with capacitive charge balance scheme for $2N$ LED strings.

further improved CLC-T circuit shown in Fig. 6 combining capacitive charge balancing can save half the number of balancing capacitors. However, the design is different from that in Fig. 5(b).

Considering the unidirectional conduction of LED loads, a rectifier and a low-pass filter are needed to provide the required dc current. A full-wave rectifier and a half-wave rectifier should be used here. In Fig. 6, half-wave rectifiers are used for the number of LED strings twice that of the charge balancing capacitors. Fig. 7 gives a hybrid structure with $(2N + M)$ LED strings for different optimized applications, where N and M can be odd or even. The input ac voltage v_{AB} is generated from a full-bridge circuit with an input dc voltage $V_{\rm IN}$, and $|v_{AB}|$ is modulated by the duty cycle D of the full-bridge circuit. An isolated transformer for safety can be incorporated into the CLC circuit as shown in Fig. 7. To achieve an accurate output constant current, the high-order harmonics of $v_{\rm AB}$ should be filtered. Essentially, the *LCLC* series-parallel resonant network has a good input higher harmonics filtering performance [27]. An additional inductor L_1 in series with an C_1 modified from the original C as shown in Fig. 7 is used for the harmonic filtering and the retention of constant output current, input ZPA and reactive current balancing scheme.

A. Selection of Balancing Capacitor

Fig. 7 uses N half-wave rectifiers and M full-rectifiers to balance $(2N + M)$ LED strings. Assume a nominal current of $I_{\rm LED}$ in each LED string. Obviously, $C_{\rm HB1} = C_{\rm HB2} = \cdots = C_{\rm HBN} = C_{\rm HB}$ and $C_{\rm FB1} = C_{\rm FB2} = \cdots = C_{\rm FBM} = C_{\rm FB}$ can balance the respective $2N$ and M LED strings. Based on the current waveforms of capacitor currents $i_{\rm CHB}$ and $i_{\rm CFB}$ drawn in Fig. 8, the averaged current $I_{\rm LED}$ can be determined as

$$I_{\rm LED} = \frac{1}{\pi} I_{\rm CHB_m} \text{ and } I_{\rm LED} = \frac{2}{\pi} I_{\rm CFB_m}. \tag{12}$$

Thus, the peak current $I_{\rm CHB_m} = 2I_{\rm CFB_m} = I_m = \pi I_{\rm LED}$. With the near identical voltage of capacitor strings, the capacitances of $C_{\rm HB}$ and $C_{\rm FB}$ should satisfy

$$C_{\rm FB} = \frac{C_{\rm HB}}{2}. \tag{13}$$

To achieve good current balancing performance, $X_{\rm CHB} = \frac{1}{\omega C_{\rm HB}} \gg \frac{4R_{\rm STR}i}{\pi^2}$ where $i \in \{1, 2, \cdots, N\}$ and $X_{\rm CFB} = \frac{1}{\omega C_{\rm FB}} \gg \frac{8R_{\rm STR}k}{\pi^2}$ where $k \in \{1, 2, \cdots, M\}$. Substituting (13) into these two equations, we have

$$X_{\rm CHB} = \frac{1}{\omega C_{\rm HB}} \gg \frac{4R_{\rm STRi}}{\pi^2} \text{ and } i \in \{1, 2, \cdots, (2N + M)\}. \tag{14}$$

To realize ZPA, the equivalent capacitance C_{eq} of the capacitor strings should satisfy (5) at the transformer primary. So

$$C_{eq} = \left(N + \frac{M}{2}\right) C_{\rm HB} \text{ and} \tag{15}$$

$$\omega = 2\pi f_s = \frac{1}{\sqrt{n^2 {\rm LC}_{eq}}} \tag{16}$$

where the transformer turns ratio is $1 : n$ and f_s is the switching frequency of the full-bridge with switches $Q_{1,2,3,4}$. Simplifying (15) and (16), we have

$$C_{\rm HB} = \frac{1}{4\pi^2 f_s^2 n^2 (N + \frac{M}{2})} \cdot \frac{1}{L}. \tag{17}$$

The voltage stresses of $C_{\rm HB}$ and $C_{\rm FB}$ are close but different. As the capacitor $C_{\rm HB}$ services the purposes of both reactive current balancing and charge balancing, it suffers from the ac voltage stress and the bias dc voltage stress between two antiparalleled LED resistances. The capacitor $C_{\rm FB}$ only suffers from the ac voltage stress. As the LED resistance is much smaller than the reactance of the balancing capacitor, the dc bias is much smaller than the ac voltage. The capacitor voltage stresses are given as follows:

$$V_{\rm CFB} = I_{\rm CFB_m} \cdot \frac{1}{\omega C_{\rm FB}} = \frac{\pi I_{\rm LED}}{\omega C_{\rm FB}} = \frac{2\pi I_{\rm LED}}{\omega C_{\rm HB}} \tag{18}$$

$$V_{\rm CHB} = I_{\rm CHB_m} \cdot \frac{1}{\omega C_{\rm HB}} + \frac{|R_{\rm STR_{(2i)}} - R_{\rm STR_{(2i-1)}}|}{2} \cdot I_{\rm LED} = I_{\rm LED} \left(\frac{2\pi}{\omega C_{\rm HB}} + \frac{|R_{\rm STR_{(2i)}} - R_{\rm STR_{(2i-1)}}|}{2}\right) \tag{19}$$

where $i \in \{1, 2, \cdots, N\}$.

B. Output Current and Control Scheme

The current of each capacitor string is in phase so that the total current in the transformer secondary $i_{\rm SEC}(t) = (N + \frac{M}{2}) \cdot i_{\rm CHB}(t)$ and the peak current is

$$I_{\rm SEC_m} = \left(N + \frac{M}{2}\right) I_{\rm CHB_m} = \left(N + \frac{M}{2}\right) \pi I_{\rm LED}. \tag{20}$$

The reflected primary current is given as

$$i_{\rm PRI} = n \cdot i_{\rm SEC} \text{ and } I_{\rm PRI_m} = n I_{\rm SEC_m}. \tag{21}$$

In Fig. 5(b), L and C resonate at f_s with constant output current and input ZPA. Here, for the purpose of higher harmonics filtering, we add L_1 and C_r in-front of the CLC-T circuit as shown in Fig. 9(a). As L_1 and C_r are designed to resonate at f_s as shown in Fig. 9(a), it has zero impedance at f_s. The circuit is reduced to Fig. 5(b) at f_s. Combining C_r and C to become C_1

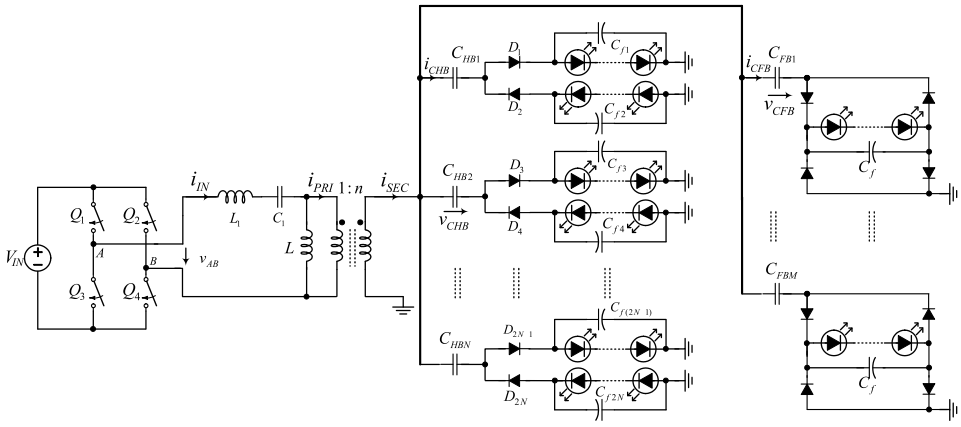

Fig. 7. Proposed LED driver based on an improved *LCLC* resonant circuit with current balancing for $(2N + M)$ LED strings.

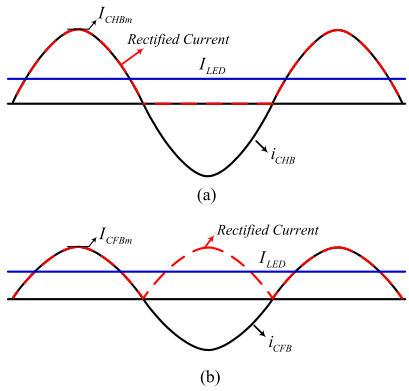

Fig. 8. Current waveforms of the balancing capacitor and the averaged current of LED string: (a) half-wave rectifier and (b) full-wave rectifier.

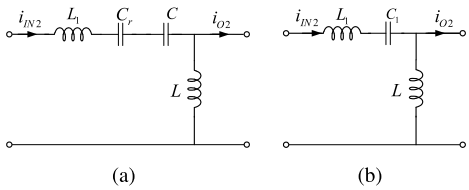

Fig. 9. Derivation of *LCLC* circuit from Fig. 5(b): (a) adding L_1 and C_r and (b) C_r and C are combined into C_1.

as shown in Fig. 9(b), we have

$$C_1 = \frac{C_r C}{C_r + C} \text{ and} \tag{22}$$

$$\omega = 2\pi f_s = \frac{1}{\sqrt{\text{LC}}} = \frac{1}{\sqrt{L_1 C_r}}. \tag{23}$$

Substituting (23) into (22), we obtain

$$\omega = 2\pi f_s = \frac{1}{\sqrt{(L + L_1)C_1}} \tag{24}$$

where L determines the output current and $L_1 C_1$ are used to filter out the high-order harmonics of the PWM-modulated voltage v_{AB}. With sufficient large L_1 and C_1, only the ac fundamental voltage v_{IN} of v_{AB} remains.

$$v_{\text{IN}}(t) = \frac{4V_{\text{IN}}}{\pi} \sin\frac{\pi D}{2} \sin(\omega t + \theta). \tag{25}$$

The output current at transformer primary is

$$i_{\text{PRI}} = \frac{v_{\text{IN}}}{j\omega L}. \tag{26}$$

Substituting (25) and (26) into (21), we have

$$L = \frac{2V_{\text{IN}} \sin\frac{\pi D}{2}}{\pi^3 f_s n(N + \frac{M}{2}) I_{\text{LED}}}. \tag{27}$$

Choosing sufficient large L_1, C_1 can be calculated by (24). Here, L_1 is usually designed a bit larger than that in (24) to permit ZVS of power switches. With L in (27), C_{HB} in (17) will become

$$C_{\text{HB}} = \frac{\pi I_{\text{LED}}}{8 f_s n V_{\text{IN}} \sin\frac{\pi D}{2}}. \tag{28}$$

From the aforementioned design, fix-frequency duty cycle control can be easily implemented by sensing only one LED string current for feedback control. The balancing capacitors C_{HB} and C_{FB} make sure the other strings having the same currents. Some commercial ICs such as UCC3895 will facilitate the control logic. With the component tolerances, the output current error is small and the variation of duty cycle can be small, and hence does not affect the realization of ZVS of the power switches.

C. Dimming and Protection

In this current balancing scheme, $2N$ LED strings are driven by a half-wave-rectified sinusoidal current at f_s and M LED strings are driven by a full-wave-rectified sinusoidal current at $2f_s$. These pulsing currents are filtered by a filtering capacitor C_f to generate an average current I_{avg} superimposed with a peak-to-peak current of $2\Delta I_{\text{avg}}$. The time constant of the parallel connected C_f and LED string is determined by the product of the LED inner dynamic resistance R_{dyn} and C_f. Usually, R_{dyn} can be as small as several ohms. The capacitor C_f will absorb the extra charge of the rectified current above I_{avg}. An integration of the current for the total charge Q above I_{avg} within a

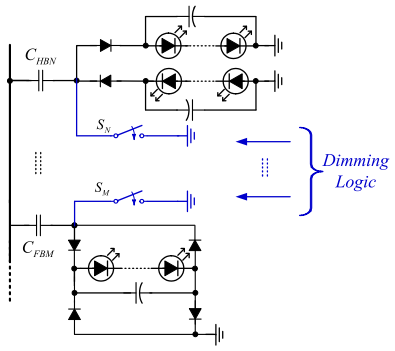

Fig. 10. LED strings with dimming switches and control logic.

current pulse period gives the magnitude $\Delta v_{C_f} = \frac{Q}{C_f}$ of the increased capacitor voltage above the averaged capacitor voltage. The ripple current magnitude $\Delta I_{\rm avg}$ can be estimated by $\frac{\Delta v_{C_f}}{R_{\rm dyn}}$. For full-bridge rectification, and using (12), we have

$$i_{\rm CFB}(t) = \frac{\pi}{2} I_{\rm CFBm} \sin \omega t - I_{\rm avgFB} \text{ and} \tag{29}$$

$$r_{\rm FB} = \frac{\Delta I_{\rm avgFB}}{I_{\rm avgFB}} = \frac{\pi \cos(\sin^{-1}\frac{2}{\pi}) - (\pi - 2\sin^{-1}\frac{2}{\pi})}{2\omega C_f R_{\rm dyn}} = \frac{0.053}{f_s C_f R_{\rm dyn}}. \tag{30}$$

For half-bridge rectification, we have

$$i_{\rm CHB}(t) = \pi I_{\rm CHBm} \sin \omega t - I_{\rm avgHB} \text{ and} \tag{31}$$

$$r_{\rm HB} = \frac{\Delta I_{\rm avgHB}}{I_{\rm avgHB}} = \frac{2\pi \cos(\sin^{-1}\frac{1}{\pi}) - (\pi - 2\sin^{-1}\frac{1}{\pi})}{2\omega C_f R_{\rm dyn}} = \frac{0.276}{f_s C_f R_{\rm dyn}}. \tag{32}$$

The minimum filtering capacitance $C_{f,\min}$ can thus be determined by the maximum allowable current ripple factor given by either (30) or (32).

PWM dimming is a better dimming method for LEDs because of simplicity. The proposed LED driver can provide an output current source for each LED string. When some LEDs or one LED string is shorted, the equivalent LED string resistance $R_{\rm STR}$ becomes small or even zero. The reactance of the balancing capacitor dominates the output current so that current balancing is still operative. However, when one LED is damaged such that the LED string is open, $R_{\rm STR}$ becomes very large. Without a current path, the current balancing is not guaranteed, and over voltage may occur that other LED strings may be damaged. Hence, an open-circuit protection must be provided for safety. The dimming switch connected in series with an LED string creates open circuit, which must be prohibited for this design. In contrast, dimming switches in parallel with LED strings will realize PWM dimming safely as shown in Fig. 10. When S is ON, the constant current flows into the dimming switch and the external voltage across the associated rectifier diodes and LED string(s) is kept zero. Since the associated rectifier diodes are reverse biased by the voltage across C_f that v_{C_f} will be discharged by the parallel connected LED loads. If S is OFF, the LED string is turned ON. The rectified $i_{\rm SEC}$ will charge C_f rapidly to the LED string forward voltage. The dimming frequency $f_{\rm dim}$ can be independent of the operating frequency of the converter. In consideration of light flicker perceived by human eyes, the dimming frequency $f_{\rm dim}$ can be set higher than 3 kHz such that even at 100% current modulation, the visual distractions such as the *phantom array* can be eliminated [28]. In practice, if we assume that the PWM-modulated current is a square pulse with duty ratio $D_{\rm dim}$ and a dimming frequency $f_{\rm dim}$, the current ripple factor after the filtration of C_f is given by

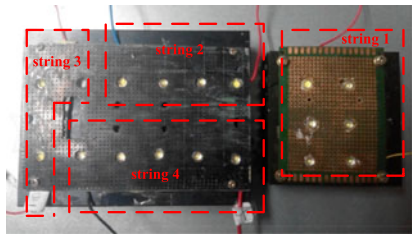

Fig. 11. Four LED strings used in the prototype.

$$r_{\rm dim} = \frac{\Delta I_{\rm avg,dim}}{I_{\rm avg,dim}} = \frac{1 - D_{\rm dim}}{2 f_{\rm dim} C_f R_{\rm dyn}}. \tag{33}$$

Hence

$$C_f = \max\left(\frac{1 - D_{\rm dim}}{2 f_{\rm dim} R_{\rm dyn} r_{\rm dim}}, C_{f\min}\right) \tag{34}$$

where $r_{\rm dim}$ is within $[0, 1]$ and can be assigned as 1 for $f_{\rm dim} \geq 3$ kHz.

Additionally, the parallel dimming circuit can be easily incorporated into open-circuit protection. If one LED string is sensed open, S is turned ON for the protection. Other LED strings can continue their normal operation.

IV. Evaluation

To verify the aforementioned analysis, a prototype LED driver has been built for driving four LED strings having a total power of up to about 20 W. The Cree Cool white XR-E series LEDs are used in this prototype [29]. Typical current of one LED is 0.35 A with $V_F = 3.3$ V at 25 °C. For a small number of balancing capacitors, $N = 2$ and $M = 0$ are selected. Two capacitors $C_{\rm HB}$ with half-wave rectifiers are used. To evaluate the current balancing performance, four LED strings having different numbers of LEDs in series are implemented, where string 1 has six LEDs, string 2 has four LEDs, string 3 has three LEDs and string 4 has five LEDs, as shown in Fig. 11. The four switching MOSFETs are driven by a phase-shift controller UCC3895. The operating frequency f_s is 90 kHz. The input voltage is a 48-V dc bus and D is designed as 0.95. The key parameters are listed in Table I.

Fig. 12 gives the waveforms of Q_1 gate voltage $v_{\rm GS1}$, bridge voltage $v_{\rm AB}$, input current $i_{\rm IN}$ and transformer secondary current $i_{\rm SEC}$ driving the four LED strings. From Fig. 12, the current $i_{\rm IN}$ is nearly in phase with v_{AB} to show that resistive

TABLE I
KEY PARAMETERS

Parameter	Value
L_1	230 μH
C_1	13 nF
L	16.5 μH
$C_{\rm HB}$	10 nF
Transformer 1:n	1:3
Switches $Q_{1,2,3,4}$	IRF540
Rectified diodes $D_{1,2,3,4}$	MBR20100CT
$C_{f\,1,2,3,4}$	110 μF

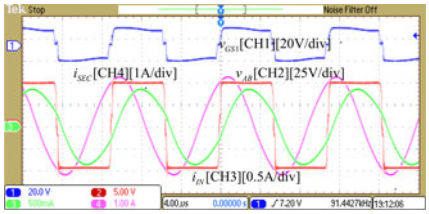

Fig. 12. Waveforms of $v_{\rm GS1}$, $v_{\rm AB}$, input current $i_{\rm IN}$ and transformer secondary current $i_{\rm SEC}$ at $V_{\rm IN} = 48$ V.

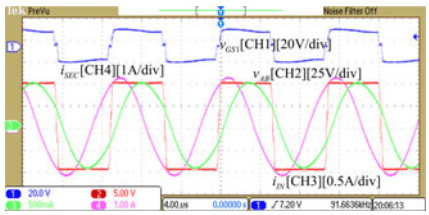

Fig. 13. Waveforms of $v_{\rm GS1}$, $v_{\rm AB}$, $i_{\rm IN}$ and $i_{\rm SEC}$ with different loads at $V_{\rm IN} = 48$ V.

input impedance eliminates most reactive power. The mostly pure sinusoidal waveform of $i_{\rm IN}$ shows that the designed *LCLC* circuit has good filter performance and the accurate output current can be ensured. The measured $i_{\rm SEC}$ agrees well with the calculation in (20). To investigate the characteristic of constant current source, LED string 3 is replaced with a large resistor via an electronic load, but still much smaller than the reactance of $C_{\rm HB}$. Fig. 13 shows the corresponding waveforms in comparison to Fig. 12. Under the same test condition and variable load, we have the same $i_{\rm SEC}$, duty cycle and phase angle between $v_{\rm AB}$ and $i_{\rm IN}$. This verifies that the output current and input impedance are independent of load variation. The small phase angle of $i_{\rm IN}$ lagging $v_{\rm AB}$ ensures the ZVS of full-bridge switches in all load range. The load-independent current source characteristic is also verified dynamically as shown in Fig. 14. When LED strings 1 and 2 are kept ON and LED strings 3 and 4 are turned OFF by controlling the dimming switch with $v_{\rm GSdim}$, the currents $i_{\rm SEC}$ and $i_{\rm CHB2}$ are maintained at their original constant steady-state currents after several switching periods with LED-load-resistance variations from $R_{\rm STR3,4}$ to zero. From Fig. 14, the magnitude of $i_{\rm CHB2}$ is always half the magnitude of $i_{\rm SEC}$, which shows the good current balancing against load variation.

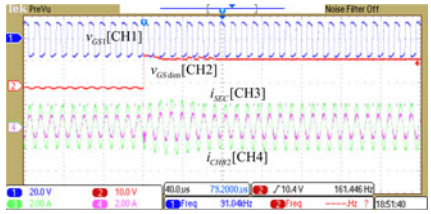

Fig. 14. Dynamic waveforms of $v_{\rm GS1}$, $v_{\rm GSdim}$, $i_{\rm SEC}$ and $i_{\rm CHB2}$ at $V_{\rm IN} = 48$ V.

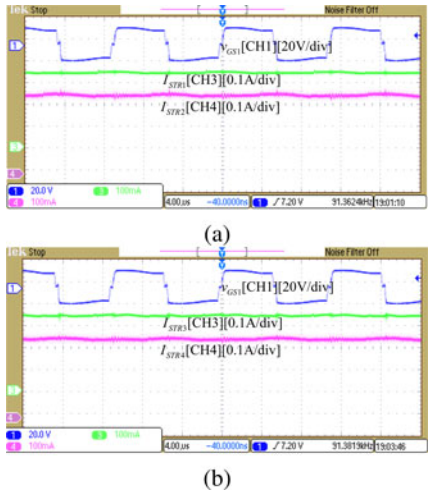

Fig. 15. Currents of four LED strings with $I_{\rm LED} = 0.35$ A. (a) For string 1 and 2. (b) For string 3 and 4.

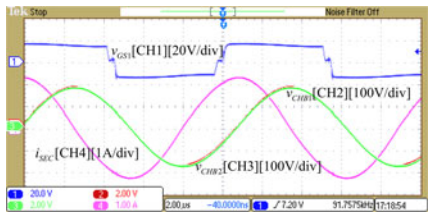

Fig. 16. Waveforms of $v_{\rm GS1}$, $i_{\rm SEC}$ and balancing capacitor voltages $v_{\rm CHB1}$, $v_{\rm CHB2}$.

Fig. 15 shows dc currents flowing across the four LED strings. With the reactance of $C_{\rm HB}$ much larger than $R_{\rm STR1,2,3,4}$, the proposed LED driver has good current balancing performance. With a well-designed *LCLC* circuit as described in Section III, each string has the required current of 350 mA. The voltage stresses of $v_{\rm CHB1}$ and $v_{\rm CHB2}$ are measured in Fig. 16. Due to the the small dc bias of every antiparalleled LED resistance, $v_{\rm CHB1}$ and $v_{\rm CHB2}$ are almost the same and close to the calculated values. This verifies the theoretical calculations. The efficiency of the LED driver is as high as 91.23 % at $V_{\rm IN} = 48$ V with the four LED strings. The main losses are magnetic conduction losses and core losses in L and the transformer, whose optimization is omitted here.

Fig. 17 gives waveforms of the main switch gate voltage $v_{\rm GS1}$, the dimming switch gate voltage $v_{\rm GSdim}$, the current i_S of the dimming switch S_2 and $I_{\rm STR4}$ of LED string 4 when

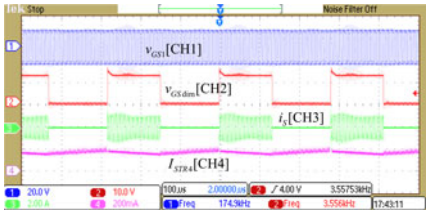

Fig. 17. Dimming-operation waveforms of v_{GS1}, v_{GSdim}, i_S and I_{STR4}.

LED strings 3 and 4 are dimmed with $D_{\mathrm{dim}} \approx 0.5$ by S_2. The current ripple factor r_{dim} is designed as 10%. The LED strings 1 and 2 are always ON. The current I_{STR3} has the same dimming waveform as I_{STR4} and is not shown in Fig. 17. To avoid light flicker, f_{dim} is chosen at 3.5 kHz. The measured current ripple is consistent with the theoretical calculation in (34).

V. Conclusion

Current balancing techniques are important for driving multiple LEDs due to device variation and heterogeneous working environment. This paper proposes an optimized *LCLC* current-source-output LED driver with capacitive current balancing to realize zero input reactive power for switching devices, constant current output independent of LED load variation and current balancing for odd or even number of LED strings. The circuit is simple, reliable, economical and efficient for multiple LED string applications. Moreover, it is inherently short-circuit proof. The switch parallel to LED string can be readily implemented with the functions of dimming and open-circuit protection. Detailed design, analysis and implementation are introduced in this paper. The experimental verifications have shown excellent agreement with the theoretical predictions.

References

[1] D. A. Steigerwald, J. C. Bhat, D. Collins, R. M. Fletcher, M. O. Holcomb, and M. J. Ludowise, "Illumination with solid state lighting technology," *IEEE J. Sel. Topics Quantum Electron.*, vol. 8, no. 2, pp. 310–320, Mar./Apr. 2002.

[2] C. Y. Wu, T. F. Wu, J. R. Tsai, Y. M. Chen, and C. C. Chen, "Multi-string LED backlight driving system for LCD panels with color sequential display and area control," *IEEE Trans. Ind. Electron.*, vol. 55, no. 10, pp. 3791–3800, Oct. 2008.

[3] X. Qu, S. C. Wong, and C. K. Tse, "Resonance-assisted buck converter for offline driving of power LED replacement lamps," *IEEE Trans. Power Electron.*, vol. 26, no. 2, pp. 532–540, Feb. 2011.

[4] Q. Hu and R. Zane, "Minimizing required energy storage in off-line LED drivers based on series-input converter modules," *IEEE Trans. Power Electron.*, vol. 26, no. 10, pp. 2887–2895, Oct. 2011.

[5] K. I. Hwu and Y. T. Yau, "Applying one-comparator counter-based sampling to current sharing control of multichannel LED strings," *IEEE Trans. Ind. Appl.*, vol. 47, no. 6, pp. 2413–2421, Nov./Dec. 2011.

[6] X. Qu, S.C. Wong, and C.K. Tse, "Non-cascading structure for electronic ballast design for multiple LED lamps with independent brightness control," *IEEE Trans. Power Electron.*, vol. 25, no. 2, pp. 331–340, Feb. 2010.

[7] W. Chen and S. Y. R. Hui, "A dimmble light-emitting diode driver with mag-amp postregualtors for multistring applicaitons," *IEEE Trans. Power Electron.*, vol. 26, no. 6, pp. 1714–1722, Jun. 2011.

[8] S. N. Li, W. X. Zhong, W. Chen, and S. Y. R. Hui, "Novel self-configurable current-miror techniques for reducing current imbalance in parallel light-emitting diode(LED) strings," *IEEE Trans. Power Electron.*, vol. 27, no. 4, pp. 2153–2162, Apr. 2012.

[9] Y. Hu and M. M. Jovanovic, "LED driver with self-adaptive drive voltage," *IEEE Trans. Power Electron.*, vol. 23, no. 6, pp. 3116–3125, Nov. 2008.

[10] H. J. Chiu, Y. K. Lo, J. T. Chen, S. J. Cheng, C. Y. Lin, and S. C. Mou, "A high-efficieny dimmable LED driver for low-power lighting applications," *IEEE Trans. Ind. Electron.*, vol. 57, no. 2, pp. 735–743, Feb. 2010.

[11] X. Qu, S.C. Wong, and C. K. Tse, "A current balancing scheme with high luminous efficacy for high-power LED lighting," *IEEE Trans. Power Electron.*, vol. 29, no. 6, pp. 2649–2654, Jun. 2014.

[12] X. Wu, Z. Wang, and J. Zhang, "Design considerations for dual-output quasi-resonant flyback LED driver with current-sharing transformer," *IEEE Trans. Power Electron.*, vol. 28, no. 10, pp. 4820–4830, Oct. 2013.

[13] J. Zhang, L. Xu, X. Wu, and Z. Qian, "A precise passive current balancing method for multioutput LED drivers," *IEEE Trans. Power Electron.*, vol. 26, no. 8, pp. 2149–2159, Aug. 2011.

[14] J. Zhang, J. Wang, and X. Wu, "A capacitor-isolated LED driver with inherent current balance capability," *IEEE Trans. Ind. Electron.*, vol. 59, no. 4, pp. 1708–1716, Apr. 2012.

[15] H. Wu, S. Ji, F. C. Lee, and X. Wu, "Multi-channel constant current (MC^3) LLC resonant LED driver," in *Proc. IEEE Energy Convers. Congr. Expo.*, 2011, pp. 2568–2575.

[16] X. Wu, J. Zhang, and Z. Qian, "A simple two-channel LED driver with automatic precise current sharing," *IEEE Trans. Ind. Electron.*, vol. 58, no. 10, pp. 4783–4788, Oct. 2011.

[17] K. I. Hwu and S. C. Chou, "A simple current-balancing converter for LED lighting," in *Proc. IEEE Appl. Power Electron. Conf.*, 2009, pp. 587–590.

[18] K. H. Jung, J. W. Yoo, and C. Y. Park, "A design of current balancing circuit for parallel connected LED strings using balancing transformers," in *Proc. IEEE Int. Conf. Power Electron.*, 2011, pp. 528–535.

[19] Y. Hu and M. M. Jovanovic, "A new current-balancing method for paralleled LED strings," in *Proc. IEEE Appl. Power Electron. Conf. Expo.*, 2011, pp. 705–712.

[20] R. Zhang and H. S. H. Chung, "Use of daisy-chained transformers for current-balancing multiple LED strings," *IEEE Trans. Power Electron.*, vol. 29, no. 3, pp. 1418–1433, Mar. 2014.

[21] S. Zhang, Q. Chen, J. Sun, M. Xu, and Y. Qiu, "High accuracy passive current balancing schemes for large-scale LED backlight system," in *Proc. IEEE Appl. Power Electron. Conf. Expo.*, 2011, pp. 723–727.

[22] X. Wu, C. Hu, J. Zhang, and C. Zhao, "Series-parallel autoregulated charge-balancing rectifier for multioutput light-emitting diode driver," *IEEE Trans. Ind. Electron.*, vol. 61, no. 3, pp. 1262–1268, Mar. 2014.

[23] S. M. Baddela and D. S. Zinger, "Parallel connected LEDs operated at high frequency to improve current sharing," in *Proc. IEEE Ind. Appl. Conf.*, 2004, pp. 1677–1681.

[24] S. Choi and T. Kim, "Symmetric current-balancing circuit for LED backlight with dimming," *IEEE Trans. Ind. Electron.*, vol. 59, no. 4, pp. 1698–1706, Apr. 2012.

[25] C. Zhao, X. Xie, and S. Liu, "Multioutput LED drivers with precise passive current balancing," *IEEE Trans. Power Electron.*, vol. 28, no. 3, pp. 1438–1448, Mar. 2013.

[26] Q. Luo, S. Zhi, C. Zou, W. Lu, and L. Zhou, "An LED driver with dynamic high-frequency sinusoidal bus voltage regulation for multistring applications," *IEEE Trans. Power Electron.*, vol. 29, no. 1, pp. 491–500, Jan. 2014.

[27] Z. Ye, P. K. Jain, and P. C. Sen, "A full-bridge resonant inverter with modified phase-shift modulation for high-frequency AC power distribution systems," *IEEE Trans. Ind. Electron.*, vol. 54, no. 5, pp. 2831–2845, Oct. 2007.

[28] B. Lehman and A. J. Wilkins, "Designing to mitigate the effects of flicker in LED lighting reducing rishs to health and safety," *IEEE Power Electron. Mag.*, vol. 1, no. 3, pp. 18–26, Sep. 2014.

[29] Cree Inc. (2009). Cree Xlamp XR-E LED data sheet [Online]. Available: http://www.cree.com/products/pdf/XLamp7090XR-E.pdf

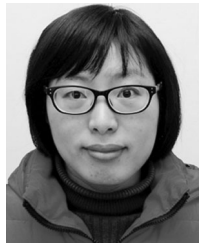

Xiaohui Qu (S'08–M'10) received the B.Sc. and M.Sc. degrees in electrical engineering from the Nanjing University of Aeronautics and Astronautics, Nanjing, China, in 2003 and 2006, respectively, and the Ph.D. degree in power electronics from the Hong Kong Polytechnic University, Hong Kong, in 2010.

From February to May 2009, she was engaged as a Visiting Scholar at the Center for Power Electronics Systems, Virginia Tech, Blacksburg, VA, USA. Since April 2010, she has been a Lecturer with the School of Electrical Engineering, Southeast University, Nanjing. Her current research interests include LED lighting systems, wireless power transfer, power-factor-correction preregulators, and resonant converters.

Siu-Chung Wong (M'01–SM'09) received the B.Sc. degree in physics from the University of Hong Kong, Hong Kong, in 1986, the M.Phil. degree in electronics from the Chinese University of Hong Kong, Hong Kong, in 1989, and the Ph.D. degree from the University of Southampton, Southampton, U.K., in 1997.

He joined the Hong Kong Polytechnic, Hong Kong, in 1988 as an Assistant Lecturer. He is currently an Associate Professor at the Department of Electronic and Information Engineering, Hong Kong Polytechnic University, where he conducts research in power electronics. He is an Editor of the *Energy and Power Engineering Journal* and a Member of the Editorial Board of the *Journal of Electrical and Control Engineering*. In 2012, he was appointed as a Chutian Scholar Chair Professor by the Hubei Provincial Department of Education, China, and the appointment was hosted by the Wuhan University of Science and Technology, Wuhan, China. In 2013, he was appointed as Guest Professor by the School of Electrical Engineering, Southeast University, Nanjing, China. He was a Visiting Scholar at the Center for Power Electronics Systems, Virginia Tech, Blacksburg, VA, USA, in November 2008, Aero-Power Sci-Tech Center, Nanjing University of Aeronautics and Astronautics, Nanjing, in January 2009, and the School of Electrical Engineering, Southeast University, Nanjing, in March 2012.

Dr. Wong is a Member of the Electrical College, Institution of Engineers, Australia.

Chi K. Tse (M'90–SM'97–F'06) received the B.Eng. (Hons.) degree in electrical engineering and the Ph.D. degree from the University of Melbourne, Melbourne, Australia, in 1987 and 1991, respectively.

He is currently the Chair Professor of Electronic Engineering at the Hong Kong Polytechnic University, Hong Kong. From 2005 to 2012, he was the Head of the Department of Electronic and Information Engineering at the same university. His research interests include complex network applications, power electronics and nonlinear systems. He serves as Editor-in-Chief for the IEEE CIRCUITS AND SYSTEMS MAGAZINE and Editor-in-Chief of IEEE CIRCUITS AND SYSTEMS SOCIETY NEWSLETTER. He was/is an Associate Editor for the IEEE TRANSACTIONS ON CIRCUITS AND SYSTEMS PART I—FUNDAMENTAL THEORY AND APPLICATIONS from 1999 to 2001 and again from 2007 to 2009. He has also been an Associate Editor for the IEEE TRANSACTIONS ON POWER ELECTRONICS since 1999. He is an Editor of *International Journal of Circuit Theory and Applications* and on the editorial boards of a few other journals.

Dr. Tse received the Best Paper Award from IEEE TRANSACTIONS ON POWER ELECTRONICS in 2001 and the Best Paper Award from *International Journal of Circuit Theory and Applications* in 2003. In 2005 and 2011, he was selected and appointed as IEEE Distinguished Lecturer. In 2007, he was awarded the Distinguished International Research Fellowship by the University of Calgary, Calgary, Canada. In 2009 and 2013, he and his coinventors won the Gold Medal at the International Exhibition of Inventions of Geneva, Switzerland, on LED lighting technologies. In 2011, he was appointed the Honorary Professor by RMIT University, Melbourne. In 2013 and 2015, he was awarded the Gledden Fellowship and the Distinguished International Fellowship by the University of Western Australia, Perth, Australia.